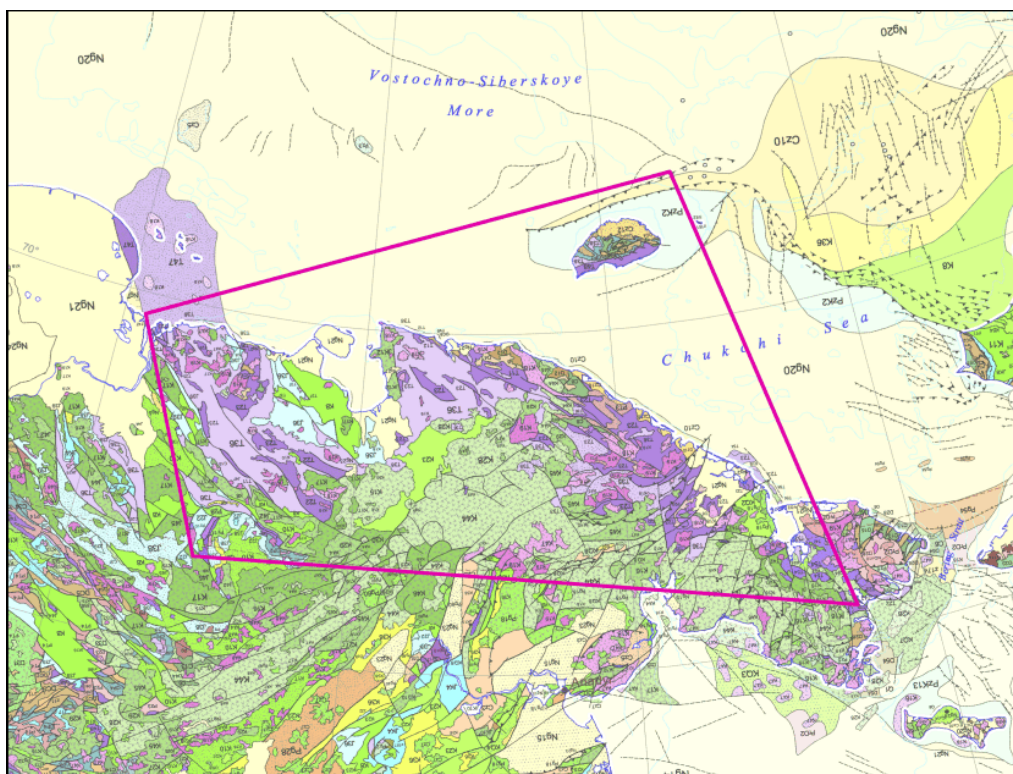


GEOLOGY OF CHUKOTKA PENINSULA AND SURROUNDING AREAS

A REGIONAL STUDY REPORT IN 2 VOLUMES



ArcGeoLink Ltd. (UK)

**IN COOPERATION WITH EXPERTS FROM GEOLOGICAL INSTITUTE (MOSCOW, RF) AND
OOO GEOLTSENTER SPBSU (ST. PETERSBURG, RF)**

GEOLOGY OF CHUKOTKA PENINSULA AND SURROUNDING AREAS

Volume 1: REGIONAL GEOLOGY

This report summarizes geological data on the onshore Chukotka Peninsula, Wrangel Island and adjacent onshore territories of the Northeastern Asia. Main purpose of this study is to provide a modern geological and tectonic framework that can be useful for companies involved in exploration for mineral resources in this vast region.

Most of the results presented in the Volume 1 are in the public domain, except for some new data that were collected by Dr. Sergey Sokolov and Dr. Marianna Tuchkova from Geological Institute of Russian Academy of Sciences (GIN RAS, Moscow) who has compiled this report. The latter consists of 163 pages including 124 illustrations.

Volume 1. Table of Contents:

EXECUTIVE SUMMARY

- 1. INTRODUCTION**
- 2. OVERVIEW OF PREVIOUS GEOLOGICAL STUDIES**
- 3. TECTONIC FRAMEWORK**
 - 3.1. New Siberian–Wrangel Fold System*
 - 3.2. Anyui–Chukotka Fold System*
 - 3.3. South Anyui Fold System (Suture Zone)*
- 4. NEW SIBERIAN–WRANGEL FOLD SYSTEM**
 - 4.1. Metamorphic complex*
 - 4.2. Paleozoic sedimentary rocks*
 - 4.3. Mesozoic sedimentary rocks*
 - 4.4. Upper Cretaceous to Cenozoic sediments*
 - 4.5. Magmatism*
- 5. ANYUI–CHUKOTKA FOLD SYSTEM**
 - 5.1. Metamorphic complex*
 - 5.2. Paleozoic sedimentary rocks*
 - 5.3. Mesozoic sedimentary rocks*
 - 5.4. Granitoid Magmatism*
 - 5.5. Gabbro–dolerite magmatism*
- 6. SOUTH ANYUI SUTURE**
 - 6.1. Tectonic-stratigraphic units*
 - 6.2. Structural observations*
 - 6.3. Ophiolites*
- 7. OVERVIEW OF PROVENANCE STUDIES**
- 8. CONCLUSION**
- 9. LIST OF REFERENCES**

List of Illustrations:

- FIGURE 1.1.** Location of the study areas.
- FIGURE 3.1.** Tectonic structure of the Northeastern Russia.
- FIGURE 3.1.1.** Photograph of conglomerates of the metamorphic complex.
- FIGURE 3.1.2.** Photograph of Upper Devonian–Lower Carboniferous polymictic conglomerates.
- FIGURE 3.1.3.** Photograph of alternating Lower–Middle Carboniferous carbonate (brown) and clayey (gray) rocks.
- FIGURE 3.1.4.** (a) Photograph of turbidites with sole marks; (b) Photograph of deformations in Triassic turbidites.
- FIGURE 3.1.5.** Photograph of Triassic rocks (dark) overthrust along a low angle thrust onto Carboniferous limestones (brownish) in the Somnitel’nyi Creek area.
- FIGURE 3.2.1.** Map of main tectonic elements of Anyui–Chukotka Fold System.
- FIGURE 4.1.1.** Geological Map of Wrangel Island.
- FIGURE 4.1.2.** Photograph of Wrangel metamorphic complex in the Tsentral’nye Mountains, Khishchnikov River.
- FIGURE 4.1.3.** Photograph of Wrangel metamorphic complex in the Tsentral’nye Mountains, Khishchnikov River.
- FIGURE 4.1.4.** Photograph of contact between Wrangel Complex (dark) and Paleozoic rocks.
- FIGURE 4.1.5.** Photograph of granite gneiss of Wrangel metamorphic complex in the Tsentral’nye Mountains, Khishchnikov River.
- FIGURE 4.2.1.** Photograph of Upper Silurian–Lower Devonian formation.
- FIGURE 4.2.2.** Photograph of brecciated limestone outcropping in junction area of the Neizvestnaya and Lemmingovaya.
- FIGURE 4.2.3.** Photograph of basal conglomerate unit of the Lower–Upper Devonian succession.
- FIGURE 4.2.4.** Photograph of outcrops of the Lower–Upper Devonian sedimentary rocks.
- FIGURE 4.2.5.** Photograph of Lower–Upper Devonian clastic rocks: fine rhythmic alternation of sandstones and shales.
- FIGURE 4.2.6.** Photographs of Lower–Middle Carboniferous succession (a), and alternating clayey shales and carbonate rocks (b).
- FIGURE 4.2.7.** Photograph of lenticular intercalations of cherts, Khishchnikov River.
- FIGURE 4.2.8.** Photograph of Lower to Middle Carboniferous alternating carbonate and clayey rocks.
- FIGURE 4.2.9.** Photograph of Calcareous–clayey laminated shales, Khishchnikov River.
- FIGURE 4.2.10.** Photograph of the Mineev overthrust nappe and its tectono-stratigraphic units.
- FIGURE 4.2.11.** Photograph of contact zone of Carboniferous calcareous sandstones and siltstones with Permian shales.
- FIGURE 4.2.12.** Photographs of exposures of Permian shale succession.
- FIGURE 4.2.13.** Photographs of exposures of the Permian rocks.
- FIGURE 4.3.1.** Photograph of imbricate–thrust structure of Triassic turbidites in the Cape Zanes area.
- FIGURE 4.3.2.** Photographs of subhorizontal thrust separating sandy (upper) and shaly (lower) Triassic units.
- FIGURE 4.3.3.** Photographs of ripple marks in Triassic sandstones.
- FIGURE 4.3.4.** Photographs of mudstone intraclasts in Triassic sandstone beds in the Khishchnikov River (a) and Chertov Ravine (b) areas.
- FIGURE 4.3.5.** Photograph of a concretion in Triassic sandstones and silty mudstones, the Khishchnikov River area.
- FIGURE 4.4.1.** Results of U–Pb dating of zircons from altered basic rocks.
- FIGURE 4.4.2.** Results of U–Pb dating of zircons from leucogranite (Sample 86-4) and granite porphyry (Sample 86-8).
- FIGURE 4.4.3.** Photograph of volcanic rocks in the middle reaches of the Neizvestnaya River.
- FIGURE 4.4.4.** Photograph of spheroidal joint in basalts, middle reaches of the Neizvestnaya River.
- FIGURE 5.1.** Stratigraphy of the Anyui–Chukotka Fold System.
- FIGURE 5.1.1.** Schematic geological map showing location of Precambrian rocks in the Chukotka Peninsula and Wrangel Island.
- FIGURE 5.1.2.** Photographs of crystalline schists (a) and marbles outcropped near Novoe Chaplino.

FIGURE 5.2.1. Schematic map showing occurrence of Paleozoic rocks in Chukotka.

FIGURE 5.2.2. Occurrence of the Paleozoic sedimentary successions in the present-day structure of the region (satellite image).

FIGURE 5.2.3. Photograph of Devonian-Lower Carboniferous and Triassic outcrops of the Alarmaut Uplift.

FIGURE 5.2.4. Schematic lithological–stratigraphic section of Paleozoic and Mesozoic rocks of the Alyarmaut Uplift (Kytep-Guitenryveem River canyon).

FIGURE 5.2.5. Schematic lithological–stratigraphic section of Paleozoic and Mesozoic rocks of the Alyarmaut Uplift.

FIGURE 5.2.6. Photograph of exposure the Upper Devonian–Lower Carboniferous rocks.

FIGURE 5.2.7. Photographs of Exposures of presumable Upper Devonian rocks.

FIGURE 5.2.8. Photograph of crystalline schists of the Lyupveem Formation.

FIGURE 5.2.9. Photographs of the lower part of the Vernitakaiveem Formation.

FIGURE 5.2.10. Photographs of the Vernitakaiveem Formation represented by gray limestones (a) alternating with quartzites (b).

FIGURE 5.2.11. Photographs of the upper Vernitakaiveem Formation, the Alyarmaut Uplift, Yagel’nyi Creek.

FIGURE 5.2.12. Photograph depicting relationships of the Devonian–Carboniferous rocks with overlying strata in the upper reaches of the Lyupveem River.

FIGURE 5.2.13. Photograph of deformation style of the Vernitakaiveem Formation, left bank of the Lyupveem River.

FIGURE 5.2.14. Photograph of deformed quartz boudines in Upper Devonian to Lower Carboniferous micaceous schists, left side of the Pogynden River (a), and contact of Upper Devonian–Lower Carboniferous schists with Lower Carboniferous limestones (b).

FIGURE 5.2.15. Geological map of the Cape Kibera area showing location of exposures of Devonian and Carboniferous rocks.

FIGURE 5.2.16. Photograph of Devonian outcrops, view from the Cape Kibera.

FIGURE 5.2.17. Photograph of Lower–Middle Devonian rocks with intense limonitization in the upper part.

FIGURE 5.2.18. Photographs of a Devonian outcrop: (a) the upper part of the section, (b) the basal part of the section.

FIGURE 5.2.19. Photographs of: (a) a mafic dike in Devonian rocks, (b) foliated Upper Devonian mudstones with cleavage.

FIGURE 5.2.20. Photographs of abundant pyrite aggregates in Devonian rocks and cavities formerly filled with its crystals.

FIGURE 5.2.21. Photographs of deformed (corrugated) quartz veins in Devonian rocks (a); Devonian rocks from the hornfelses zone (b).

FIGURE 5.2.22. Photographs of the Lower Carboniferous polymictic conglomerates cropped out on Cape Kibera.

FIGURE 5.2.23. Photographs of: (a) alternating gravelites and detrital limestones with distinct contacts between them; (b) Dark gray limestones with thin lenticular intercalations of gray limestones.

FIGURE 5.2.24. Photograph of Light green detrital limestones alternating with sandy limestones.

FIGURE 5.2.25. Photograph of a tectonic contact of Carboniferous limestones overthrust onto Permian–Triassic clastic rock unit.

FIGURE 5.2.26. Location of the Kus’veem River in the Chukchi Peninsula.

FIGURE 5.2.27. Photograph of an outcrop of marbles, calcareous and muscovite–chlorite schists, Matlyu Peninsula, Novoe Chaplino Settlement.

FIGURE 5.3.1. Correlation scheme of Triassic sedimentation cycles in Western Chukotka.

FIGURE 5.3.2. Fragments of Lower–Middle Triassic sedimentary section cropped out in the Enmyneem River banks.

FIGURE 5.3.3. Photographs of siderite concretions in Lower–Middle Triassic sedimentary rocks.

FIGURE 5.3.4. Photographs of exposures of the Upper Triassic rocks of the Chukotka Peninsula.

FIGURE 5.3.5. Photographs of exposures of Norian formations.

FIGURE 5.3.6. Photographs of Upper Triassic Norian siliciclastic succession.

FIGURE 5.3.7. Photographs of deformations in Upper Triassic rocks.

- FIGURE 5.3.8.** Photographs of exposures of basal part of the Permian–Triassic section.
- FIGURE 5.3.9.** Photograph of a Carnian unit of alternating thin sandstone and silty mudstone, Ergyvaam River bank.
- FIGURE 5.3.10.** Schematic correlation between Triassic sections along the southern margin of the Chukotkan microcontinent.
- FIGURE 5.3.11.** Photographs of Lower–Middle Triassic section along Ploskaya River bank.
- FIGURE 5.3.12.** Location map of Jurassic-Cretaceous depressions.
- FIGURE 5.3.13.** Location map of Cretaceous facial zones.
- FIGURE 5.3.14.** Correlation chart for the Upper Jurassic-Lower Cretaceous sedimentary successions of the Chukotka Peninsula.
- FIGURE 5.3.15.** Photograph of exposure of the Jurassic–Cretaceous Rauchua Formation overlying the Upper Triassic strata.
- FIGURE 5.3.16.** Photographs of mudstone intraclasts in sandstones of the Rauchua Formation.
- FIGURE 5.3.17.** Photograph of slump folds in alternating mudstones and siltstones of the Netpneiveem Formation.
- FIGURE 5.3.18.** Photograph of lenses of tuff-conglomerates of the Imlekynsk formation (Tithonian).
- FIGURE 5.3.19.** Photograph of exposure of pebbly clay unit of the Imlekynsk Formation in the left bank of the Glukhaya River.
- FIGURE 5.3.20.** Photograph of outcrops revealing relationship between Jurassic and Cretaceous rocks.
- FIGURE 5.3.21.** Photograph of gradational bedding in the Pogyden Formation sandstone.
- FIGURE 5.3.22.** Photographs Berriasian–Valanginian siliciclastic succession cropping out in coastal cliffs of Chaun Bay.
- FIGURE 5.3.23.** Photograph of Berriasian–Valanginian rocks with a metamorphosed coal seam.
- FIGURE 5.3.24.** Photograph of a coal quarry, Ol'khovaya Formation.
- FIGURE 5.3.25.** Photographs of Upper Cretaceous effusive rocks of the Okhotsk-Chukotka Volcanic Belt.
- FIGURE 5.4.1.** Location map of Chukotka showing occurrences of granite massifs.
- FIGURE 5.4.2.** Schematic geological map of central Chukotka.
- FIGURE 5.4.3.** Geological map of the Cape Kibera area.
- FIGURE 5.4.4.** Concordia Diagram for zircons from granitic rocks of the Kibera Massif and Kuekvun Massif.
- FIGURE 5.4.5.** The Tera–Wasserburg plots for granitoids of the Alyarmaut Uplift.
- FIGURE 5.4.6.** $F2/F1$, $Rb/Y+Nb$, and $FeO^*/MgO-Zr+Nb+Ce+Y$ diagrams for granitoid rocks of the Alyarmaut Uplift.
- FIGURE 5.5.1.** Schematic geological map of the Malyi Anyui Uplift (Western Chukotka).
- FIGURE 5.5.2.** Schematic geological map of an area of a dolerite body occurrence in the Paleozoic–Triassic Keverveem Formation.
- FIGURE 5.5.3.** Schematic geological map of the Kal'khaurveem River valley, Koluchinskaya Estuary area, eastern Chukotka.
- FIGURE 5.5.4.** Results of U–Pb TIMS dating of magmatic zircons from gabbro from the Kal'khaurveem River valley.
- FIGURE 5.5.5.** Photograph of a tectonic block of ultramafic and mafic rocks within volcanic rocks of the Okhotsk–Chukotka Volcanic Belt.
- FIGURE 5.5.6.** Photograph of metasomatic transformation of ultramafic rocks confined to steep tectonic contacts of serpentized spinel peridotites.
- FIGURE 5.5.7.** Photograph of metasomatic (?) leucocratic rocks within serpentized spinel peridotites.
- FIGURE 6.1.** Map of tectono-stratigraphic units of western Chukotka.
- FIGURE 6.1.1.** Tectono-stratigraphic chart of the South Anyui Terrane.
- FIGURE 6.1.2.** Photograph of an exposure of the Flysch Unit.
- FIGURE 6.1.3.** Panoramic view of the South Gremuchinsky accretionary wedge unit.
- FIGURE 6.2.1.** Diagram illustrating Stage 1 deformation in gabbro rocks.
- FIGURE 6.2.2.** Thrust-style deformations in clastic rocks of the Lower-middle Devonian Ustieva unit.
- FIGURE 6.2.3.** Schematic geological cross-section across the Penveem Uplift.
- FIGURE 6.3.1.** Photographs of an outcrop of the Aluchin ophiolite (dunite–harzburgite) complex.

- FIGURE 6.3.2.** Photographs of: (a) spinel dunite (dunite–harzburgite complex), and (b) banded gabbro (cumulative complex).
- FIGURE 7.2.1.** Photograph of a thin-section of a Carnian metasandstone.
- FIGURE 7.2.2.** Schematic geological map of the Malyi Anyui River basin.
- FIGURE 7.2.3.** Circum-Arctic map showing the location of Triassic detrital zircon samples and the main tectonic features of the Arctic Basin.
- FIGURE 7.2.4.** Relative probability distribution diagrams for detrital zircon U-Pb ages from Triassic sandstones of Wrangel Island.
- FIGURE 7.2.5.** Geologic map of the Khichshnikov River region, Wrangel Island.
- FIGURE 7.2.6.** Relative age probability distribution diagrams for 0–3000-Ma detrital zircon grains from stratigraphic units of Wrangel Island.
- FIGURE 7.2.7.** Location of sampling sites for detrital zircons from Triassic and Jurassic–Cretaceous successions of the Anyui Subterrane.
- FIGURE 7.2.8.** Relative probability distribution diagram for detrital zircon U-Pb ages from Triassic sandstones of Chukotka.
- FIGURE 7.2.9.** Cumulative age probability curves and relative probability distribution diagrams (inset) for detrital zircon ages.
- FIGURE 7.3.1.** Geological map of the Uyamkanda River area.
- FIGURE 7.3.2.** (a)-(c) distribution plots of fission-track ages of zircon grains from samples 9947, 9947/1, and 9986.
- FIGURE 8.1.** Interpreted seismic reflection profile across the North Chukchi Basin.

GEOLOGY OF CHUKOTKA PENINSULA AND SURROUNDING AREAS

Volume 2: PROVENANCE, PALEOGEOGRAPHY & UPLIFT HISTORY

The Volume 2 is the final product of the implemented regional study of the Chukotka Peninsula. It summarizes the results of analytical investigations of samples from Paleozoic and Mesozoic sedimentary rocks of the Chukotka Peninsula, which include U-Pb detrital zircon geochronology, whole-rock Sm-Nd isotopic and chemical studies, X-Ray diffraction of mudstone rocks, apatite and zircon fission track studies, vitrinite reflectance, Rock-Eval studies and thin-section description. The main goals of these studies were (i) obtaining new modern analytical data from several key sedimentary sections that would allow for more accurate constraint of the geologic history of the region, and (ii) producing a model of tectonic and sedimentary evolution of the region with reference to events that may affect the offshore South and North Chukchi sedimentary basins.

The Volume 2 consists of 107 pages including 76 illustrations. The information about the used samples and raw analytical data are provided in 9 attachments. The Volume 2 is accompanied by an ArcGIS database.

Volume 2. Table of Contents:

EXECUTIVE SUMMARY

1. INTRODUCTION

2. TECTONIC FRAMEWORK

3. SEDIMENT PROVENANCE STUDY

3.1. Petrology of sedimentary rocks

3.1.1. Devonian

3.1.2. Carboniferous

3.1.3. Triassic

3.1.4. Jurassic-Cretaceous

3.2. U–Pb detrital zircon dating

3.3. Sm–Nd isotopic composition of sedimentary rocks

3.4. Geochemistry of sedimentary rocks

3.5. Provenance and paleogeography reconstruction

4. ORGANIC MATTER MATURITY AND COMPOSITION

4.1. Post-depositional rocks transformations based on X-ray investigations

4.2. Vitrinite reflectance data

4.3. Rock-Eval data

5. MAIN PHASES OF UPLIFT, COOLING AND EROSION

5.1. Apatite fission-track (AFT) results

5.2. Zircon fission-track (ZFT) results

6. CONCLUSIONS

LIST OF REFERENCES

ATTACHMENTS

Volume 2. List of Illustrations:

- FIGURE 1.1.** Main tectonic elements of the Anyui-Chukotka Fold System.
- FIGURE 2.1.** Schematic tectonic map of the Northeastern Asia.
- FIGURE 2.2.** Stratigraphy of the Anyui–Chukotka Fold System.
- FIGURE 2.3.** Location of the Upper Jurassic-Lower Cretaceous syn-collisional depressions.
- FIGURE 2.4.** Schematic terrane map of the Koryak Highland.
- FIGURE 2.5.** Stratigraphy of Devonian-Cretaceous succession of the Anyui subterrane, Western-Chukotka terrane.
- FIGURE 2.6.** Stratigraphy of Devonian-Cretaceous succession of the Chaun subterrane, Western-Chukotka terrane.
- FIGURE 2.7.** Stratigraphy of Carboniferous-Cretaceous succession of the Chaun subterrane (Velmay River).
- FIGURE 3.1.** Geologic map of the Chukotka Peninsula showing location of the field study areas.
- FIGURE 3.1.1.** Thin section images of Devonian sandstone (Cape Kibera).
- FIGURE 3.1.2.** Thin section images of Carboniferous sandstone (Cape Kibera).
- FIGURE 3.1.3.** Thin-section images of Triassic sandstones.
- FIGURE 3.1.4.** Mineral composition of Triassic sandstones.
- FIGURE 3.1.5.** Argillite intraclasts in sandstones of the Rauchua Formation.
- FIGURE 3.1.6.** Thin-section images of Upper Jurassic-Lower Cretaceous arkose sandstones.
- FIGURE 3.1.7.** Mineral composition of Triassic sandstones.
- FIGURE 3.1.8.** Thin-section images of sandstones from the Upper Jurassic Netpneiveem Formation.
- FIGURE 3.1.9.** Thin-section images of sandstones of the Jurassic-Cretaceous succession from the Pevék Depression.
- FIGURE 3.2.1.** Location of detrital zircon samples in the Anyui-Chukotka Fold System.
- FIGURE 3.2.2.** Relative age probability distribution plots for detrital zircon grains from Triassic siliciclastic rocks.
- FIGURE 3.2.3.** Relative age probability distribution plots for detrital zircon grains from Lower-Middle Triassic siliciclastic rocks of the Anyui-Chukotka Fold System.
- FIGURE 3.2.4.** Relative age probability distribution plots for detrital zircons grains from Upper Triassic siliciclastic rocks of the Anyui-Chukotka Fold System.
- FIGURE 3.2.5.** Relative age probability distribution plots for detrital zircon grains from the South-Anyui terrane.
- FIGURE 3.2.6.** Relative age probability distribution plots for detrital zircon grains from Rauchua and Pevék depressions.
- FIGURE 3.2.7.** Location of sandstone samples in the Ust-Bel’skie Mountains.
- FIGURE 3.2.8.** Relative age probability distribution plots for detrital zircon grains from the Ust-Bel’skie Mountains.
- FIGURE 3.3.1.** Location of Sm-Nd samples of siliciclastic rocks in the Anyui-Chukotka Fold System.
- FIGURE 3.3.2.** Sm-Nd isotopic system in Mesozoic siliciclastic rocks of the Anyui-Chukotka Fold System.
- FIGURE 3.3.3.** Sm-Nd isotopic system in Triassic and Jurassic-Cretaceous siliciclastic rocks.
- FIGURE 3.4.1.** Location of geochemical samples of siliciclastic rocks in the Anyui-Chukotka Fold System.
- FIGURE 3.4.2.** Sandstone classification diagram (Pettijohn et al. 1987) showing composition of major rock components.
- FIGURE 3.4.3.** A-CN-K diagram (Nesbitt and Young, 1984) showing compositions for sandstones from the Anyui-Chukotka Fold System.
- FIGURE 3.4.4.** Th vs. Th/U plots for the sedimentary rock samples.
- FIGURE 3.4.5.** Al-Ti-Zr diagram (wt. %) of samples from the Anyui-Chukotka Fold System
- FIGURE 3.4.6.** Th/Sc vs. Zr/Sc diagram.
- FIGURE 3.4.7.** Provenance composition diagram for the Chukotka sedimentary rocks (after Roser and Korsch 1988).
- FIGURE 3.4.8.** Diagrams (after Taylor and McLennan, 1988) illustrating compositions of inferred source areas for sandstones of the Anyui–Chukotka Fold System.
- FIGURE 3.4.9.** Th-Sc diagram for samples from the Anyui-Chukotka Fold System.
- FIGURE 3.4.10.** Co/Th vs. La/Sc diagram for siliciclastic rocks of the Anyui-Chukotka Fold System.
- FIGURE 3.4.11.** La/Th vs. Hf diagram showing mixed felsic/basic source of siliciclastic rocks of the Anyui-Chukotka Fold System.
- FIGURE 3.4.12.** Th/Co vs. La/Sc diagram showing felsic provenance for siliciclastic rocks of Anyui-Chukotka Fold System.
- FIGURE 3.4.13.** Rare Earth elements plots for Devonian to Jurassic-Cretaceous siliciclastic rocks of the Anyui-Chukotka Fold System.
- FIGURE 3.4.14.** Eu/Eu* vs. Gdn/Ybn diagram for siliciclastic rock of the Anyui-Chukotka Fold System.
- FIGURE 3.5.1.** Schematic paleogeographic map for Early Devonian time.
- FIGURE 3.5.2.** Schematic paleogeographic map for Carboniferous time.
- FIGURE 3.5.3.** Schematic paleogeographic map for Permian-Triassic time.

- FIGURE 3.5.4.** Schematic paleogeographic map for Early Jurassic time.
- FIGURE 3.5.5.** Schematic paleogeographic map for Jurassic time.
- FIGURE 3.5.6.** Schematic paleogeographic map for Early Cretaceous time.
- FIGURE 4.1.1.** Location of Rock-Eval and Vitrinite reflectance samples.
- FIGURE 4.1.2.** Distribution of clay minerals in Devonian rocks.
- FIGURE 4.1.3.** Composition of chlorite in Paleozoic-Mesozoic rocks of the Anyui-Chukotka Fold System.
- FIGURE 4.1.4.** Distribution of clay minerals in Carboniferous rocks.
- FIGURE 4.1.5.** Distribution of clay minerals in Permian-Triassic rocks.
- FIGURE 4.1.6.** Quartz veins in the Norian sandstone unit, western spurs of the Pyrkanai Range.
- FIGURE 4.1.7.** Distribution of clay minerals in Triassic rocks.
- FIGURE 4.1.8.** Distribution of clay minerals in Upper Jurassic-Lower Cretaceous rocks.
- FIGURE 4.1.9.** Diagram illustrating variations in the illite crystallinity index (ICI) vs. the chlorite crystallinity index (CCI) for Chukotka mudstone rocks.
- FIGURE 4.1.10.** Common mesodiagenetic pathways for clay minerals in sandstones.
- FIGURE 4.1.11.** Composition of clay minerals in mudstones of the Anyui-Chukotka Fold System (X-ray diffraction).
- FIGURE 4.1.12.** Berriasian–Valanginian rocks with a metamorphosed coal seam, coastal cliffs of the Chaun Bay.
- FIGURE 4.1.13.** Sample 465/1, fragment of organic matter.
- FIGURE 4.1.14.** Correlation between the illite crystallinity index (KI) and vitrinite reflectance (Ro) for Jurassic samples.
- FIGURE 4.1.15.** Comparison of the illite Kübler index (IC) ‘crystallinity’ zones and coal rank in the very low- and low-grade metamorphic rocks.
- FIGURE 5.1.1.** Location of AFT and ZFT samples.
- FIGURE 5.1.2.** AFT thermal evolution diagram for the Lower-Middle Triassic sample B1-7 (1395-27).
- FIGURE 5.1.3.** AFT thermal evolution diagram for the Upper Triassic (Carnian) sample 422 (1395-33).
- FIGURE 5.1.4.** AFT thermal evolution diagram for the Upper Triassic (Carnian) sample 417/6 (1395-31).
- FIGURE 5.1.5.** AFT thermal evolution diagram for the Upper Triassic (Carnian) sample 453/1 (1395-29).
- FIGURE 5.1.6.** AFT thermal evolution diagram for the Upper Triassic (Norian) sample 454/1 (1395-28).
- FIGURE 5.1.7.** AFT thermal evolution diagram for the Upper Jurassic (Oxfordian-Kimmeridgian) sample 470/6 (1395-32).
- FIGURE 5.1.8.** AFT thermal evolution diagram for the Upper Jurassic (Oxfordian-Kimmeridgian) sample 456/10 (1395-30).
- FIGURE 5.2.1.** Plots demonstrating distribution of the ZFT ages for Triassic rocks of the Anyui and Chaun subterranean (samples B-1-5, 417-4, 06-12-005).
- FIGURE 5.2.2.** Plots demonstrating distribution of the ZFT ages for the rocks of the Anyui and Chaun subterranean (samples 318 and 452-6-3).
- FIGURE 5.2.3.** Plots demonstrating correlation between ZFT ages and U content in zircon grains.
- FIGURE 6.1.** Tectonostratigraphy of the Chukotka and Northern Slope of Alaska.

Volume 2. List of attachments (MS Excel Format):

Attachment 1: List of samples

Attachment 2: Zircon U-Pb ages lab data

Attachment 3: Sm-Nd composition lab data

Attachment 4: Whole-rock geochemistry lab data

Attachment 5: ICP-MS composition lab data

Attachment 6: XRD clay mineralogy lab data

Attachment 7: Apatite Fission Track lab data

Attachment 8: Zircon Fission Track lab data

Attachment 9: Rock-Eval lab data

Enquiries:

Project Leader: Dr. Sergey Drachev

sdrachev@arcgeolink.com

Ph: +44 7595 986571

ArcGeoLink Ltd. 48 Tupwood
Gardens, Caterham, Surrey CR3 6EW
UK